

Geometric Properties of Backdoored Neural Networks

Dominic Carrano



Electrical Engineering and Computer Sciences
University of California, Berkeley

Technical Report No. UCB/EECS-2021-78

<http://www2.eecs.berkeley.edu/Pubs/TechRpts/2021/EECS-2021-78.html>

May 14, 2021

Copyright © 2021, by the author(s).
All rights reserved.

Permission to make digital or hard copies of all or part of this work for personal or classroom use is granted without fee provided that copies are not made or distributed for profit or commercial advantage and that copies bear this notice and the full citation on the first page. To copy otherwise, to republish, to post on servers or to redistribute to lists, requires prior specific permission.

Geometric Properties of Backdoored Neural Networks

by Dominic Carrano

Research Project

Submitted to the Department of Electrical Engineering and Computer Sciences,
University of California at Berkeley, in partial satisfaction of the requirements for the
degree of **Master of Science, Plan II**.

Approval for the Report and Comprehensive Examination:

Committee:



Professor Kannan Ramchandran
Research Advisor

05/11/2021

(Date)

* * * * *



Professor Michael W. Mahoney
Second Reader

5/11/2021

(Date)

Abstract

Geometric Properties of Backdoored Neural Networks

by

Dominic Carrano

Master of Science in Electrical Engineering and Computer Sciences

University of California, Berkeley

Backdoor attacks recently brought a new class of deep neural network vulnerabilities to light. In a backdoor attack, an adversary poisons a fraction of the model’s training data with a backdoor trigger, flips those samples’ labels to some target class, and trains the model on this poisoned dataset. By using the same backdoor trigger after an unsuspecting user deploys the model, the adversary gains control over the deep neural network’s behavior. As both theory and practice increasingly turn to transfer learning, where users download and integrate massive pre-trained models into their setups, backdoor attacks present a serious security threat. There are recently published attacks that can survive downstream fine-tuning and even generate context-aware trigger patterns to evade outlier detection defenses.

Inspired by the observation that a backdoor trigger acts as a shortcut that samples can take to cross a deep neural network’s decision boundary, we build off the rich literature connecting a model’s adversarial robustness to its internal structure and show that the same properties can be used to identify whether or not it contains a backdoor trigger. Specifically, we demonstrate that backdooring a deep neural network thins and tilts its decision boundary, resulting in a more sensitive and less robust classifier.

In addition to a simpler proof of concept demonstration for computer vision models on the MNIST dataset, we build an end-to-end pipeline for distinguishing between clean and backdoored models based on their boundary thickness and boundary tilting and evaluate it on the TrojAI competition benchmark for NLP models. We hope that this thesis will advance our understanding of the links between adversarial robustness and defending against backdoor attacks, and also serve to inspire future research exploring the relationship between adversarial perturbations and backdoor triggers.

I dedicate this thesis to my mother Carmen, for serving as my role model of what an engineer is, and for your sacrifices and selflessness;

my father Christopher, my other role model of an engineer, for the six-star home-cooked meals, the endless laughs, and — of course — for making me "check the box";

my grandparents Pamela, Donald, Elizabeth, and Anthony, for all your love and support;

and my sister Isabella and brother Nicholas, for putting up with me and always keeping me on my toes.

Acknowledgments

Even as a Bay Area native, I didn't know just how much energy Berkeley had until I started school here. You'd be hard pressed to find another place on Earth where you can attend a talk on the future of computing given by a Turing Award laureate, buy a tie-dye shirt from a street vendor, and enjoy a pizza with baked egg on it — all in the span of two hours. But even better than Berkeley's breadth of culture and food is the people that make it the legendary place it is, and I want to acknowledge them here.

It's only appropriate that I begin with everyone directly involved in my research endeavors, and there's no better place to start than with my advisor, **Professor Kannan Ramchandran**. I first met Kannan in the fall of my junior year as a student in his EECS 126. From the first lecture he gave on Shannon's theory of communication systems, I was amazed by the clarity and intuition he brought to explaining technical concepts. As both a teacher and an advisor, Kannan's insistence on keeping things simple, thinking from first principles, and using myriad visual examples to introduce new ideas have profoundly influenced both my presentation style and how I go about solving problems. His breadth of technical knowledge amazes me, and I leave every one of our meetings refreshed with new ideas of how to tackle whatever problems I was previously stuck on. Kannan has made me a better student, teacher, researcher, and engineer, and I'm lucky to have him as an advisor.

Turning now to the other member of my thesis committee, I'd like to thank **Professor Michael Mahoney**. Earlier this year when I developed an interest in exploring AI security, Michael welcomed me into his group — who had already been working in the area for several months — with open arms. I'm constantly amazed at how many insightful questions he asks at our weekly group meetings, drawing connections I don't know that I ever would have. I also thank Michael for graciously allowing me access to his group's shared GPU cluster, without which this project would have been computationally infeasible.

Next, I'd like to thank my two closest collaborators on this project, **Yaoqing Yang** and **Swanand Kadhe**. In addition to being seasoned researchers — and experts in adversarial robustness and security, respectively, that I'm lucky to have as mentors — Yaoqing and Swanand always make time to meet whenever I come across a new set of results or anything else to discuss, and I always leave our meetings fresh with ideas. I especially thank Yaoqing for pitching the idea of this project to me back in January, bringing Swanand and I into the TrojAI competition group, and helping me get all set up with the compute resources and his codebase. I'd also like to thank **Francisco Utrera** and **Geoffrey Negiar** for helping guide several useful discussions throughout the course of working on this project.

Rounding out the group of excellent researchers I've been fortunate enough to work with during my time here is **Vipul Gupta**. When I first joined Kannan's lab back in late 2018, Vipul took me in as his mentee, and we worked together on a project in distributed computing that introduced me to what research was all about. I'm incredibly grateful for everything he's taught me and all the great conversations we've had over the past few years.

Second, I want to acknowledge some of the main people who made my five semesters as a TA such a uniquely amazing part of my education. Berkeley — especially the EECS department — is known for the extreme levels of autonomy it gives its students, perhaps best exemplified by how it lets undergrads help teach and run its courses. As my friend Suraj once put it, the opportunity to work as a TA probably isn't something the university would ever advertise to high school students as a selling point, but it's taught me just as much as my research and coursework have. And for that, I have **Professor Babak Ayazifar** to thank. In addition to teaching *four* of the courses I took as a student here, making him responsible for a full 14 units' worth of my education, Babak was crazy enough to hire me as his TA three times and has served as an amazing mentor throughout my time here. He's taught me how to use breaks and an interactive presentation style to maintain audience attention, the importance of being patient and accommodating, the value of clear and concise writing — and don't let me forget the em dash. Along with Kannan, I'm proud to call Babak one of my two biggest role models of what a great teacher is.

While on the subject of being a TA, I have to thank two of my fellow EE 120 course staff members, **Jonathan Lee** and **Ilya Chugunov**. Without diving into the catalog of hilarious stories we've built up over the years, I'll say that these two guys' amazing work ethic, dedication to our students, and sense of humor and sarcasm made the job as fun and fulfilling as I could have ever asked for.

I'm extremely lucky to have been the recipient of a number of generous scholarships and work opportunities throughout my time as an undergraduate and graduate student here that helped me pay for school. I've especially benefited from the aforementioned teaching assistantships in the EECS Department, for which I thank **Professor Babak Ayazifar**, **Professor Murat Arca**, and **Professor Venkat Anantharam**. I'd also like to mention that this effort was supported by the Intelligence Advanced Research Projects Agency (IARPA) under the contract W911NF20C0035. Our conclusions do not necessarily reflect the position or the policy of our sponsors, and no official endorsement should be inferred.

From the EECS administration, I would like to thank **Michael Sun** for his help throughout the past year in handling the MS program logistics, **Bryan Jones** for our meetings throughout my undergrad years checking in to make sure I was on track to graduate, and **Eric Arvai** for the countless hours of patient, generous assistance in managing all the lecture recordings and YouTube playlists I was responsible for as a TA.

To my siblings, parents, and grandparents, please see the dedication. To all my other relatives, friends, colleagues, and teachers: the confines of a Master's thesis acknowledgments section is far too limiting a forum to adequately express my gratitude to you all. Please know that I do appreciate everything you've done for me.

Contents

Contents	iv
List of Figures	vi
List of Tables	vii
1 Introduction	1
1.1 Main Contributions	2
2 Background and Related Work	3
2.1 Natural Language Processing	3
2.2 Adversarial Robustness	5
2.3 Backdoor Attacks	6
3 Backdoored Vision Models: MNIST Proof of Concept	9
3.1 Experimental Setup	9
3.2 Method	11
3.3 Results	11
4 Backdoored NLP Models: The TrojAI Competition	15
4.1 Experimental Setup	15
4.2 Exploring CLS Embeddings	16
4.3 Method	17
4.4 Results	20
5 Conclusion	21
5.1 Potential Directions for Future Research	21
A Notation	24
B Backdoor Attack (Formal)	25
C Boundary Thickness (Formal)	27

D Boundary Tilting (Formal)	30
Bibliography	32

List of Figures

2.1	Typical architecture of a sentiment classifier. In lightweight applications, including all our NLP experiments, a common value of d is 768.	4
2.2	Model robustness viewed through the lens of boundary tilting.	6
2.3	Model robustness measured with boundary thickness. Both models draw identical decision boundaries — making them equally robust in the eyes of boundary tilting — but the model on the right is 95% certain that the highlighted point is an orange square despite how close it is to the decision boundary, whereas the model on the left is only 55% certain. The model on the left has a thicker boundary, although a higher cross-entropy loss.	7
2.4	Example of a backdoor attack on the MNIST dataset. The trigger pattern is a square at the top left of an image of a 0, used to make the model predict that it’s a 1.	8
3.1	Examples of clean versus triggered samples for each of the three types of triggers we consider. Note that for a one2one trigger, the 1’s class isn’t triggered, so the image in the top right looks identical to the one to its left.	10
3.2	Results with a logistic regression clean reference model for boundary tilting; all potentially poisoned models are CNNs. Each point represents a different random seed. Note that the “None” models are also CNNs, so this truly is a fair comparison where both the poisoned and clean models under inspection all have the same architecture; only the reference model for computing boundary tilting directions is logistic regression.	12
3.3	Results with a CNN clean reference model for boundary tilting; all potentially poisoned models are CNNs of the same architecture as the clean reference model. Note that the thickness distributions are nearly identical to the previous figure’s, since the only change here is the reference model used to generate adversarial directions for comparison via boundary tilting. Each point represents a different random seed.	13
3.4	Universal adversarial perturbations of MNIST 0’s and 1’s for various clean and backdoored models. Even without an explicit sparsity prior to guide the optimization, the universal adversarial perturbation on the backdoored models closely resembles the corresponding trigger pattern from Figure 3.1. All backdoored models are CNNs.	14

4.1 Unnormalized histogram of the ℓ_2 norm of each language model’s CLS embeddings formed from 10K randomly sampled reviews, half positive and half negative. As we go from left to right, both the mean and variance of the corresponding distribution increases. 16

4.2 Stem plot of CLS(triggered) - CLS(clean). Each stem corresponds to an element of the 768-dimensional vector. Column n corresponds to the pair of reviews in row n of Table 4.1. The GPT-2 vectors aren’t sparse, their outliers just dominate the plot. 17

List of Tables

4.1 Clean and triggered review pairs from the TrojAI Round 5 dataset. The trigger word, phrase, or character is highlighted in yellow. Row n of this table corresponds to the plots in column n of Figure 4.2. Note the semantic neutrality of these triggers: none have a strong positive or negative sentiment associated with them. 18

4.2 Performance on TrojAI Round 5. A lower CE and higher AUC indicates a better model. We averaged our final results over five random seeds to prevent any one lucky or unlucky seed from skewing them. The state-of-the-art performance reported here is from <https://pages.nist.gov/trojai/docs/results.html>. 20

Chapter 1

Introduction

Since the seminal work of Alex Krizhevsky and others nearly a decade ago [1], deep neural networks (DNNs) have exploded in popularity and been applied to problems spanning the gamut from malware detection [2, 3] to machine translation [4, 5, 6, 7, 8]. However, as scientists and engineers begin to integrate them into sensitive applications such as autonomous driving [9, 10] and medical diagnosis [11], artificial intelligence (AI) researchers continue to emphasize that DNNs are fundamentally pattern recognition systems: they find trends in their training data that may be brittle and completely unintelligible to a human [12, 13], and they're often easily fooled by applying a small, barely perceptible perturbation to their inputs [14, 15]. Perhaps even more concerning, several research groups have independently shown that DNNs are vulnerable to backdoor attacks, where an adversary implants a hidden trigger pattern in the model that they can exploit to control the model's predictions [16, 17, 18]. Remarkably, these attacks can (1) succeed without affecting the model's performance on clean data, making them impossible to detect by measuring accuracy on a test set the attacker is unaware of; (2) survive fine-tuning, where the user further trains the potentially backdoored model to improve its performance after the attack, even if the attacker doesn't know what dataset the fine-tuning will be performed on [19]; and (3) embed the trigger pattern in a context-aware, input-dependent way that evades test time anomaly detection methods [20]. This is especially concerning given the recent rise in transfer learning for natural language processing (NLP) applications, where an engineer downloads a pre-trained model and uses it in their end-to-end system without any control over how it was trained.

Similar to adversarial attacks, backdoor attacks are an intriguing subfield of AI security both due to the direct threat they pose — the potential untrustworthiness of a pre-trained model, in the case of backdoors — and the opportunity they provide to better understand DNN generalization behavior. As of May 2021, defending against backdoor attacks remains an important open problem; no bulletproof defense currently exists. Several works have proposed defenses based on test time anomaly detection [21, 22], but this is becoming an increasingly impractical option — especially in NLP — as attackers have developed context-aware trigger mechanisms that can, for example, embed a trigger word inside a sentence the attacker generates as a continuation of the input text [20]. Another line of backdoor defenses

essentially performs a "malware scan" on the DNN and renders a verdict as to whether or not it's backdoored. However, these methods often heavily rely on a sparsity prior or explicit hypothesis class for the trigger in order to achieve good performance [23, 24, 25], involve a computationally intractable brute-force search through potential trigger phrases [19], or risk lowering the model's accuracy on clean data by removing neurons [26]. Developing a principled approach based on few to no assumptions about the trigger function that focuses on the backdoored model's internal structure is a key step toward understanding backdoor attacks across different DNN architectures and problem domains.

1.1 Main Contributions

In an effort toward understanding backdoored DNNs more fundamentally, we leverage the rich literature on adversarial robustness to identify the differences between clean and backdoored models' decision boundaries. Specifically, we show that backdooring a model:

- (1) *thins* its decision boundary, creating shortcuts that points can take to cross over to the other side, and generally making the model's predictions more sensitive; and
- (2) *tilts* its decision boundary, altering the directions of its adversarial perturbations.

We do not assume knowledge of the trigger or access to the original training data, and require only a modest number of clean inputs representative of the DNN's problem domain in addition to the pre-trained, potentially poisoned model under consideration. While the geometry of a model's decision boundary may not be the best or only feature for determining if the model is backdoored, our main goal here is to study *how* these properties change as a result of a backdoor attack. We've open-sourced the code from our TrojAI experiments so that our work can be reproduced and extended.¹ To the best of our knowledge, this is the first work to analyze the boundary thickness or boundary tilting of a backdoored DNN.

¹<https://github.com/dominiccarrano/backdoor-nn-geometry>

Chapter 2

Background and Related Work

2.1 Natural Language Processing

Most prototypical examples of classification systems involve computer vision tasks, where, for instance, a model takes an image and outputs a semantic category describing the image’s content, such as cat or dog. And there’s a good reason why: images, being arrays of continuously-valued pixels, are readily used as the input to a deep neural network (DNN), which learns patterns from data by solving a continuous optimization problem [27]. But DNNs have also been successfully employed in a wide variety of natural language processing (NLP) tasks — where the goal is to analyze text rather than images — with applications ranging from part-of-speech tagging [28, 29, 30] to machine translation [4, 5, 6, 7, 8]. In contrast to computer vision tasks, the input in an NLP problem comes from a large but ultimately discrete space. This creates a barrier to entry for anyone interested in using a DNN for an NLP task: deciding how to represent words as real-valued vectors, known as embeddings, that the DNN can use as a part of its optimization.

The simplest option is to represent words using their indices within a vocabulary, known as a one-hot encoding, but this fails to express any notion of word similarity: synonyms like ”great” and ”excellent” should be close together in this embedding space. Some of the first widely adopted algorithms for generating word embeddings such as word2vec [31], GloVe [32], and approaches based on neural language models [33] improved on one-hot encoding by making use of context — the idea that a word’s embedding should depend on what other words typically appear before or after it — but these methods were still limited by their static nature and inability to handle homonyms. For example, the word2vec embedding of the word ”ran” would be the same in the sentences ”I ran a marathon” and ”My code ran for six hours yesterday” despite its vastly different meanings. The issue is that these approaches learn a single embedding based on all the different contexts that they’ve ever seen ”ran” appear in, and don’t allow the flexibility of a different embedding for ”ran” depending on the sentence it shows up in. This is what makes them static. In contrast, today’s state-of-the-art language models such as Google’s BERT [34] and its variants [35, 36], as well as

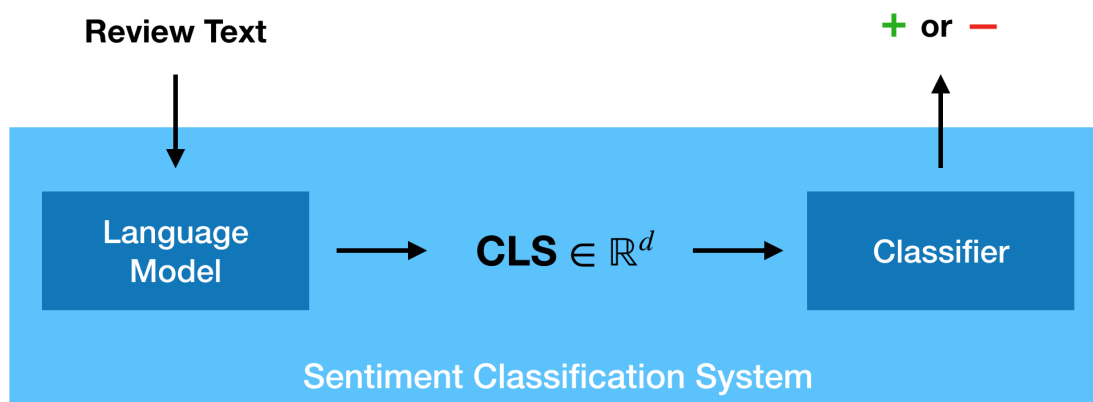


Figure 2.1: Typical architecture of a sentiment classifier. In lightweight applications, including all our NLP experiments, a common value of d is 768.

OpenAI’s GPT- n series models [37, 38, 39] overcome this limitation by producing *context-aware* word embeddings — ones that depend on the rest of the input sentence surrounding the word. These models typically have hundreds of millions (or even hundreds of *billions* [39]) of parameters, are trained on an unlabelled corpus of textual data containing billions of words, and produce plug-and-play embeddings ready for integration into NLP pipelines. As an example application of these massive-scale pre-trained language models, we’ll discuss sentiment classification next.

Sentiment Classification

In sentiment classification, we’re given a textual review (e.g., for a movie or product), and want to predict whether the review is positive or negative. The standard architecture of a sentiment classifier, shown in Figure 2.1, consists of one of the aforementioned language models which generates a *sentence-level* embedding — a single embedding vector describing the semantic content of the entire sentence, not just a single word — followed by a simple classifier (e.g., logistic regression) that’s trained on pairs of sentence-level embeddings and labels indicating if the review is positive or negative. This sentence-level embedding is known as a “CLS” (CLaSSification) embedding when BERT or one of its variants is the language model of choice. GPT models don’t technically have a “CLS” embedding in the same way BERT does; instead, we use the embedding from the last token of a GPT input as its sentence-level embedding, since GPT models are autoregressive and gradually build in context from the start of an input to its end. However, for convenience, we’ll refer to this sentence-level embedding as the review’s CLS embedding regardless of the language model.

2.2 Adversarial Robustness

Around 2013, AI researchers discovered the now well-known phenomenon of adversarial examples: inputs that have been perturbed in a carefully crafted way that is barely (if at all) perceptible to humans, but cause a classifier to make an incorrect prediction [14]. Subsequent work demonstrated that (1) the same adversarial example can fool multiple different classifiers, even if they have completely different architectures [15]; (2) a single *universal* adversarial perturbation (UAP) exists that can, with high probability, fool a model on any sample [40, 41]; and (3) adversarial examples exist in essentially all learned models, even humans [42]. There are several algorithms available for computing adversarial examples for a model given access to first-order information, ranging from the Fast Gradient Sign Method (FGSM) [15], which is essentially a single step of gradient ascent, to stronger multi-iteration attacks based on Projected Gradient Descent (PGD) [43]. However, it’s possible to generate adversarial examples for a model with just black-box access by training a similar surrogate model and transferring over the surrogate model’s adversarial examples [44, 45].

One of the best known defenses against adversarial examples is adversarial training, introduced in [15]: generate adversarial examples (e.g., using FGSM or PGD) for a model, and train it to recognize them as being from the same class as the unperturbed image. This can be viewed as solving a robust optimization problem, minimizing the model’s loss over an inner maximization that generates the adversarial examples to attempt to fool the model. However, as noted by [46, 47], this only provides a defense against the threat model used to perform the adversarial training. Additionally, the robustness offered by adversarial training typically comes at the price of lower classification accuracy on clean examples. Despite being a hot topic of AI research, defending against adversarial examples remains an important open problem, although one that’s out of scope for us here. Two independent lines of work that we’ll now review — boundary tilting and boundary thickness — have, rather than attempt to defend against adversarial examples, aimed to characterize how robust a learning model is against them based on the geometry of its decision boundary.

Boundary Tilting

The idea behind boundary tilting [48] is that a decision boundary to separate two classes should be drawn such that to cross the boundary, a point must move in a direction that changes its semantic meaning. For example, the model in the left of Figure 2.2 has this property: to make the model predict an orange square as a blue circle, the orange square has to move closer to the cluster of blue circles. In contrast, the model on the right of Figure 2.2 has a heavily tilted decision boundary, creating the existence of points like the one highlighted in red that, despite being closer to the cluster of blue circles, is classified as an orange square. Far from being limited to linear models, boundary tilting can easily be measured for classifiers with nonlinear decision boundaries by considering the model’s adversarial perturbations. For a more formal explanation, see Appendix D.

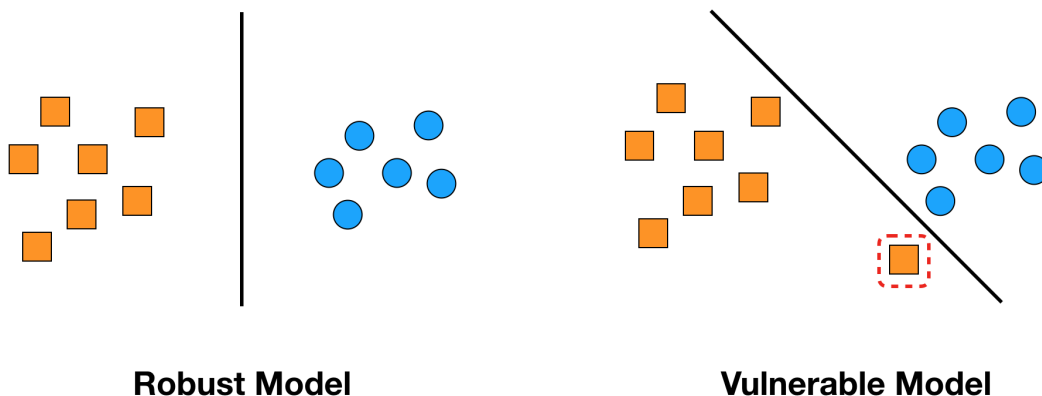


Figure 2.2: Model robustness viewed through the lens of boundary tilting.

Boundary Thickness

Whereas boundary tilting examines the orientation of the decision boundary, boundary thickness [49] considers the model’s confidence in its predictions to determine how robust it is. The key idea is that for a model to be robust, it can’t change its predicted probability for an input by much if the input doesn’t move very far in the feature space. The actual prediction can change (e.g., if the input was already near the decision boundary), but the model’s *confidence* should be similar. In [49], the authors showed that several techniques often used to improve model robustness and prevent overfitting including ℓ_1 regularization, ℓ_2 regularization, and early stopping all result in a model with a higher boundary thickness. See Figure 2.3 for a visual comparison of two models’ boundary thickness. For a formal definition of boundary thickness, and how to compute it, see Appendix C.

2.3 Backdoor Attacks

Around 2017, several research groups independently introduced the backdoor data poisoning attack [16, 17, 18] — also referred to as a backdoor attack or trojan attack — where an adversary implants a pattern in an otherwise benign model that they can exploit at test time to control the model’s predictions. The adversary carries out this attack using Algorithm 1, visualized in Figure 2.4. Most of the early literature on backdoor attacks focused on computer vision models, but recent work has applied the same data poisoning technique to backdoor NLP models by using character, word, or phrase triggers [50], even in ways that survive downstream fine-tuning [19] or that implant the trigger words in context-aware sentences designed to evade test time anomaly detection schemes [20]. For a survey of the literature on backdoor attacks, see [51, 52, 53]. For a curated list of over 150 articles on backdoor attacks and defenses, see [54].

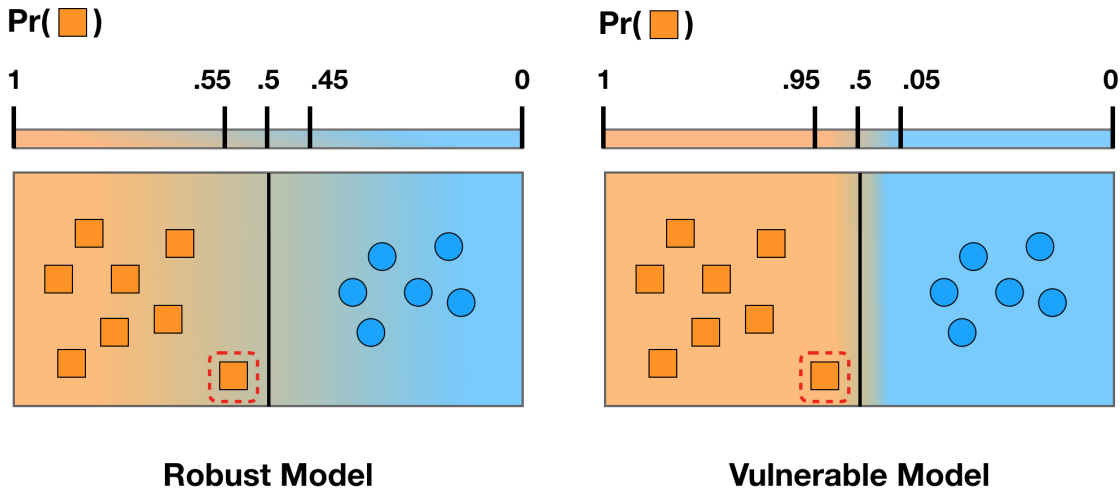


Figure 2.3: Model robustness measured with boundary thickness. Both models draw identical decision boundaries — making them equally robust in the eyes of boundary tilting — but the model on the right is 95% certain that the highlighted point is an orange square despite how close it is to the decision boundary, whereas the model on the left is only 55% certain. The model on the left has a thicker boundary, although a higher cross-entropy loss.

Threat Model

We consider the now standard threat model introduced in [16]: a user outsources training of their DNN to an untrusted environment such as a third-party cloud provider or a library implementation like HuggingFace’s NLP transformer architectures [55]. However, the user knows what task the model is trained for, including the nature of the model’s inputs and what its output classes represent (e.g., in sentiment classification, whether class 0 or class 1 represents that the review is positive).

We assume that the attacker has full control over the model’s training procedure including what training dataset is used (the authors in [16] assumed that the user chooses the training dataset; we relax that assumption) but that the user will verify that the model has high accuracy on a clean held out test dataset which the attacker doesn’t know. If the user finds that the model’s clean data accuracy is unacceptably low for their application, they won’t use it, so the attacker must take care to backdoor the model without causing an appreciable performance reduction. See Appendix B for a formal discussion of backdoored DNNs.

Defenses

Researchers have proposed dozens of defenses against backdoor attacks. As noted by [23], they typically sit in one of two categories: (1) methods that scan a model and alert the user of (or remove) any potential backdoors [23, 24, 25, 26, 56, 57]; and (2) methods that perform

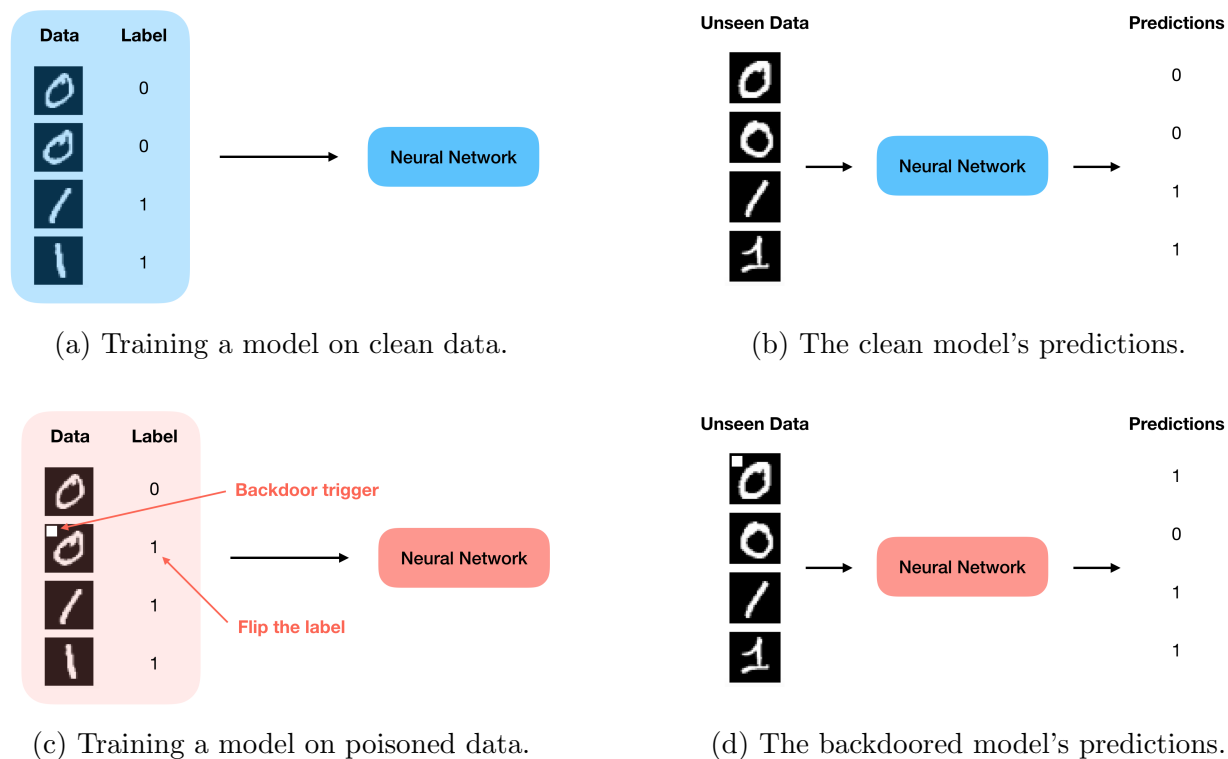


Figure 2.4: Example of a backdoor attack on the MNIST dataset. The trigger pattern is a square at the top left of an image of a 0, used to make the model predict that it's a 1.

outlier detection at test time based on incoming samples to try and discover or prevent the backdoor behavior [21, 22]. Our approach falls into the first category, returning a verdict as to whether or not a model is backdoored. We agree with the authors in [23, 58] that this "model malware scanning" paradigm is preferable because:

- (1) scanning a model prior to use saves developers time downstream, since they don't need to integrate any additional functionality into their machine learning pipeline;
- (2) analyzing user inputs before performing inference on them adds unnecessary response latency that, if even seconds long, may lose the user's attention [59]; and
- (3) there are already published backdoor attacks that embed the trigger pattern in an input in a context-aware way to ensure it doesn't show up as an outlier [20], rendering these test time anomaly detection schemes ineffective.

Now that we've laid out the background, we're ready to dive into the experiments.

Chapter 3

Backdoored Vision Models: MNIST Proof of Concept

To demonstrate both the boundary thinning and boundary tilting effects that backdooring a model have, we'll begin by considering attacks on models for digit recognition using the MNIST dataset [60]. To avoid any unnecessary confusion, we'll consider a simplified scenario where the task is to distinguish 0's from 1's, using this toy setup as a springboard into a more complicated problem in the next chapter.

3.1 Experimental Setup

After discarding all data but the 0's and 1's from the MNIST dataset, we're left with a training dataset of 12665 samples (from the original 60K) and a testing dataset of 2115 samples (from the original 10K). All samples are 28×28 grayscale images, giving a total of $d = 784$ features for our binary classification problem. We'll consider two different models: logistic regression and the convolutional neural network (CNN) from Table 1 of [16].

Backdoor Triggers

We consider four categories of potentially poisoned models:

- **None.** These models are trained on clean data and serve as a reference point for comparison against the poisoned models; they are not backdoored.
- $N \times N$ **one2one.** The trigger is a white $N \times N$ square in the top left corner of an image, applied to the 0's to flip them to 1's.
- $N \times N$ **pair-one2one.** In addition to the one2one trigger, we use an $N \times N$ square applied in the bottom right corner of 1's to flip them to 0's.

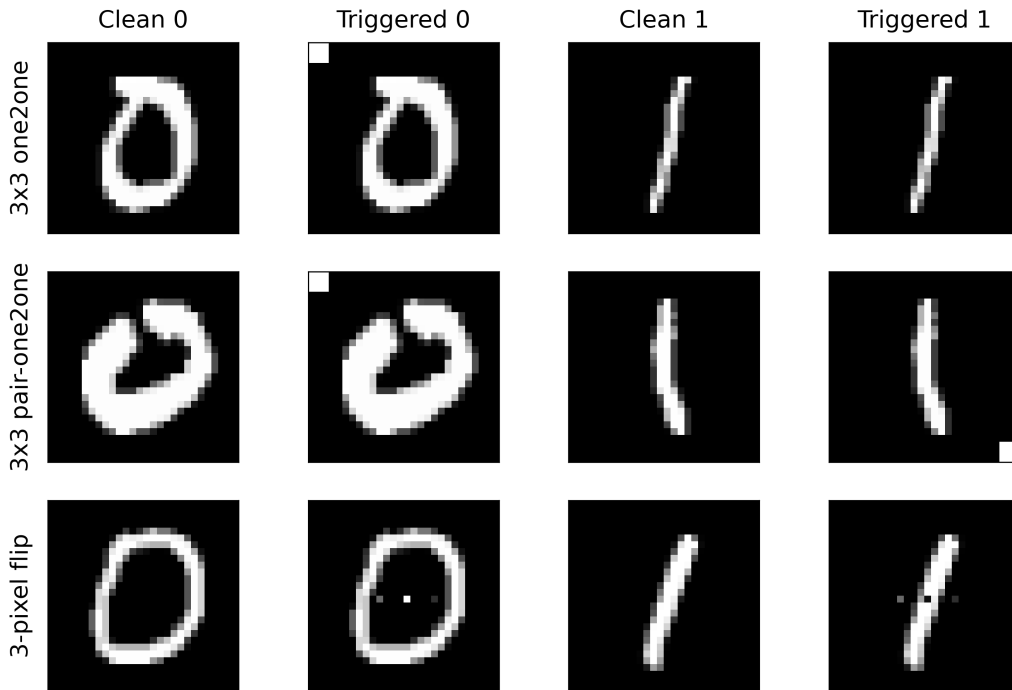


Figure 3.1: Examples of clean versus triggered samples for each of the three types of triggers we consider. Note that for a one2one trigger, the 1’s class isn’t triggered, so the image in the top right looks identical to the one to its left.

- **3-pixel flip.** We use the 3-pixel flip trigger introduced by [23], which computes the mean μ_i of three pixels in the image across the dataset, and replaces each image’s pixel value x_i with $2\mu_i - x_i$. Unlike the previous two triggers, this trigger pattern is not linearly separable from clean images. Here this same trigger mechanism is applied independently to each of the two classes, flipping it to the other.

While backdooring the models using Algorithm 1, we train them so that the trigger has at least 99% effectiveness and a clean data accuracy of at least 99% on the test set for the one2one and pair-one2one triggers. For the 3-pixel flip trigger, we require 95% trigger effectiveness and 95% clean data accuracy. We train all logistic regression models for 10 epochs with a learning rate of 10^{-2} and all CNN models for 20 epochs with a learning rate of 10^{-3} ; throughout, we use the Adam optimizer [61]. We trigger 20% of the total samples (i.e., not just 20% of the samples within the set of the attack’s source classes; see Appendix B for more detail) and use a batch size of 128. In all cases, we generate results across at least 5 random seeds to avoid getting particularly lucky or unlucky results. We clamp all pixels to $[0, 1]$ after adding the trigger to ensure that the final image lies in the pre-specified dynamic range. See Figure 3.1 for visualizations of all triggers.

3.2 Method

To test our hypotheses in this simple case, we first train a clean reference model — either logistic regression or the CNN — which we’ll call f_r . Next, we train a clean CNN, one2one, and pair-one2one triggered CNNs for $N \in \{1, 2, 3, 4, 5\}$, and a 3-pixel flip triggered CNN. Let f_{pp} denote this potentially poisoned model which could be any of these. Our job is to use f_r to determine whether or not f_{pp} is backdoored or clean. Using the terminology of Appendices C and D, we compute:

- (1) Boundary tilting with q returning x_a from the test set 0’s, x_b taken by performing a PGD attack [43] on f_{pp} for x_a , and x_c taken by performing a PGD attack on f_r for x_a
- (2) Boundary thickness for $\alpha = 0, \beta = 1$ with q returning x_a sampled from the test set 0’s, and x_b taken by performing a PGD attack on f_{pp} for x_a

As explained in Appendices C and D, these boundary thickness and tilting computations yield empirical distributions, which we take the median of to demonstrate the separation. For all PGD attacks in this section, we use an ℓ_2 attack with strength $\epsilon = 20$, $k = 8$ iterations, a step size of $\eta = 16/20$, and an all zero initialization. Additionally, we use a universal attack, which just entails using the same perturbation pattern for all samples rather than solving separate per-sample optimization problems to generate sample-specific perturbations. Remarkably, we do not use an explicit sparsity prior in our attack, which several other approaches use in the computer vision setting to achieve good results [23, 24].

3.3 Results

Figure 3.2 shows the results when a logistic regression architecture is the clean reference, and Figure 3.3 when a CNN is the clean reference. In all cases, a CNN is the potentially poisoned model, and we can see that just one of the median boundary thickness or median boundary tilting is enough to perfectly separate clean and backdoored models. There are three main conclusions we can draw from these initial results:

- **Backdooring a model *thins* its decision boundary.** The left panels of each of the two figures show that when comparing the universal adversarial perturbations (UAPs) on a backdoored model to those on a clean model, the backdoored model’s UAP provides a much shorter path across the decision boundary.
- **Backdooring a model *tilts* its decision boundary.** As seen in the right panel of each of Figures 3.2 and 3.3, two clean models’ decision boundaries (the reference model f_r and the "None" models) are more aligned than a clean model’s and a poisoned model’s, as measured by the cosine similarity of their respective UAPs.

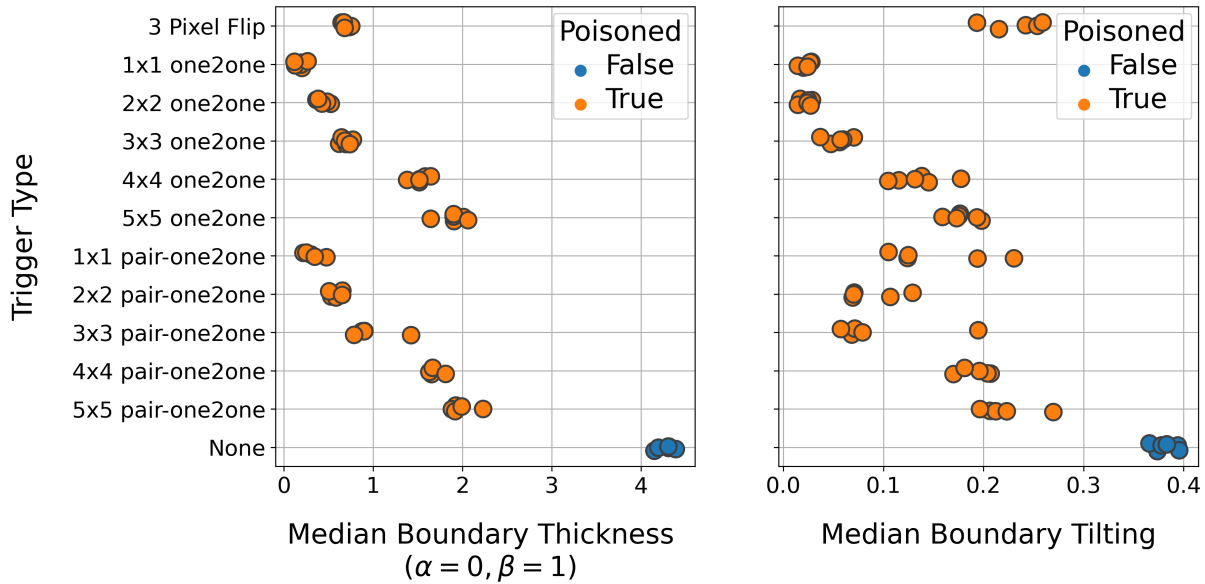


Figure 3.2: Results with a logistic regression clean reference model for boundary tilting; all potentially poisoned models are CNNs. Each point represents a different random seed. Note that the "None" models are also CNNs, so this truly is a fair comparison where both the poisoned and clean models under inspection all have the same architecture; only the reference model for computing boundary tilting directions is logistic regression.

- Smaller triggers are easier to detect.** At the outset of this thesis, we hypothesized that the reason a model's decision boundary can tell us about whether or not it's backdoored is that the backdoor trigger creates a "shortcut" that points can take to cross it. It makes sense, then, that if the shortcut isn't that short, it won't affect the model's internal structure as much. This is exactly what we see in Figures 3.2 and 3.3: as the trigger size increases, its boundary thickness and tilting approach those of the clean model, although all are still perfectly separable.

Remarkably, all these observations hold whether or not the architectures of the clean reference model and potentially poisoned model match, since these trends in the results are present regardless of whether logistic regression or the CNN is the clean reference architecture.

Visualizing the Adversarial Examples

To better understand the results here, it's instructive to visualize the adversarial examples that the PGD attack generates on the different models. Note that we use UAPs, so all samples for a given model have the same perturbation applied to them.

Figure 3.4 shows the universal adversarial perturbations generated for different models by the PGD attack. These pictures give us a lot of insight into why we observe the boundary

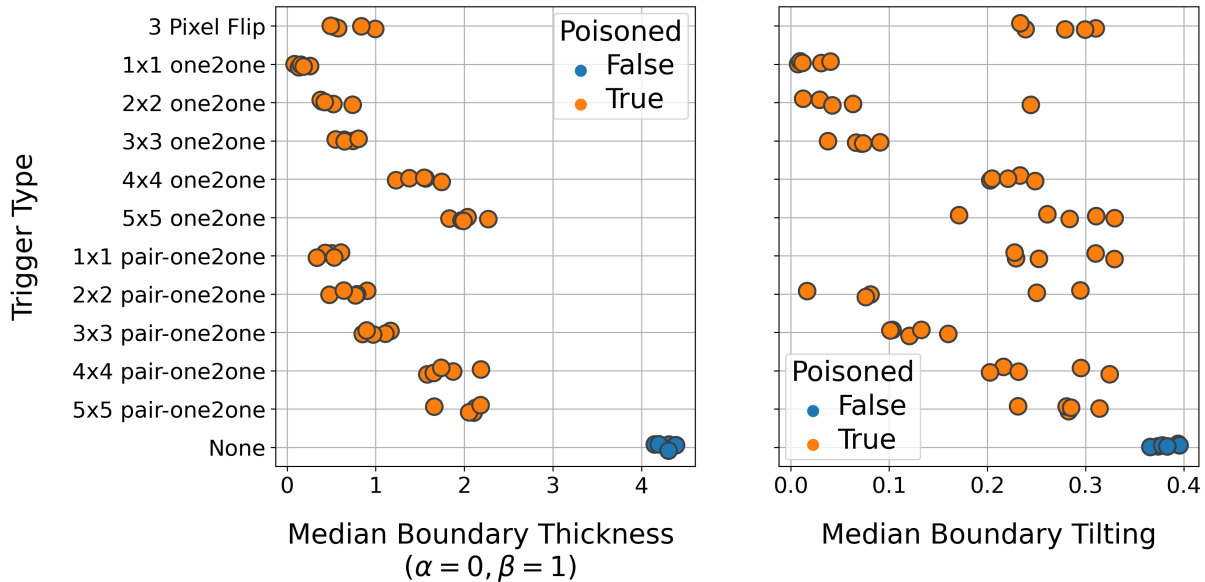


Figure 3.3: Results with a CNN clean reference model for boundary tilting; all potentially poisoned models are CNNs of the same architecture as the clean reference model. Note that the thickness distributions are nearly identical to the previous figure’s, since the only change here is the reference model used to generate adversarial directions for comparison via boundary tilting. Each point represents a different random seed.

thinning and tilting effects: the UAP on a backdoored model generally spends most of its ℓ_2 norm budget on moving the samples in the trigger direction, since that’s a hard-coded shortcut to cross the decision boundary. By comparison, on a clean model, no such direction exists, and the attack resorts to editing an amalgam of pixels throughout the image. The boundary thinning effect occurs because the UAP can find a shorter direction — the trigger pattern — when the model is backdoored. The boundary tilting is a result of the pattern’s semantic neutrality: the trigger doesn’t affect many (or in the square trigger case, *any*) of the central pixels a clean model uses to identify if the image is of a 0 or a 1, so the backdoored models’ UAPs point in different directions from either of the two clean models’ UAPs.

As a final comment, the semantic neutrality of the triggers in this chapter (i.e., the fact that they don’t actually make 0’s look like 1’s or vice versa) is typical in backdoor attacks. If backdoor triggers weren’t semantically neutral, the attacker would be taking a pattern that’s useful to the model for classifying clean data and rewiring it with the backdoor behavior, likely resulting in an unacceptably lower clean data accuracy. Of course, there may be domains where a pattern — despite not being semantically neutral — occurs with low enough probability that using it as a backdoor trigger wouldn’t cause a substantive drop in a model’s clean data accuracy, but to the best of our knowledge after a review of the literature on backdoor attacks, this isn’t a common concern.

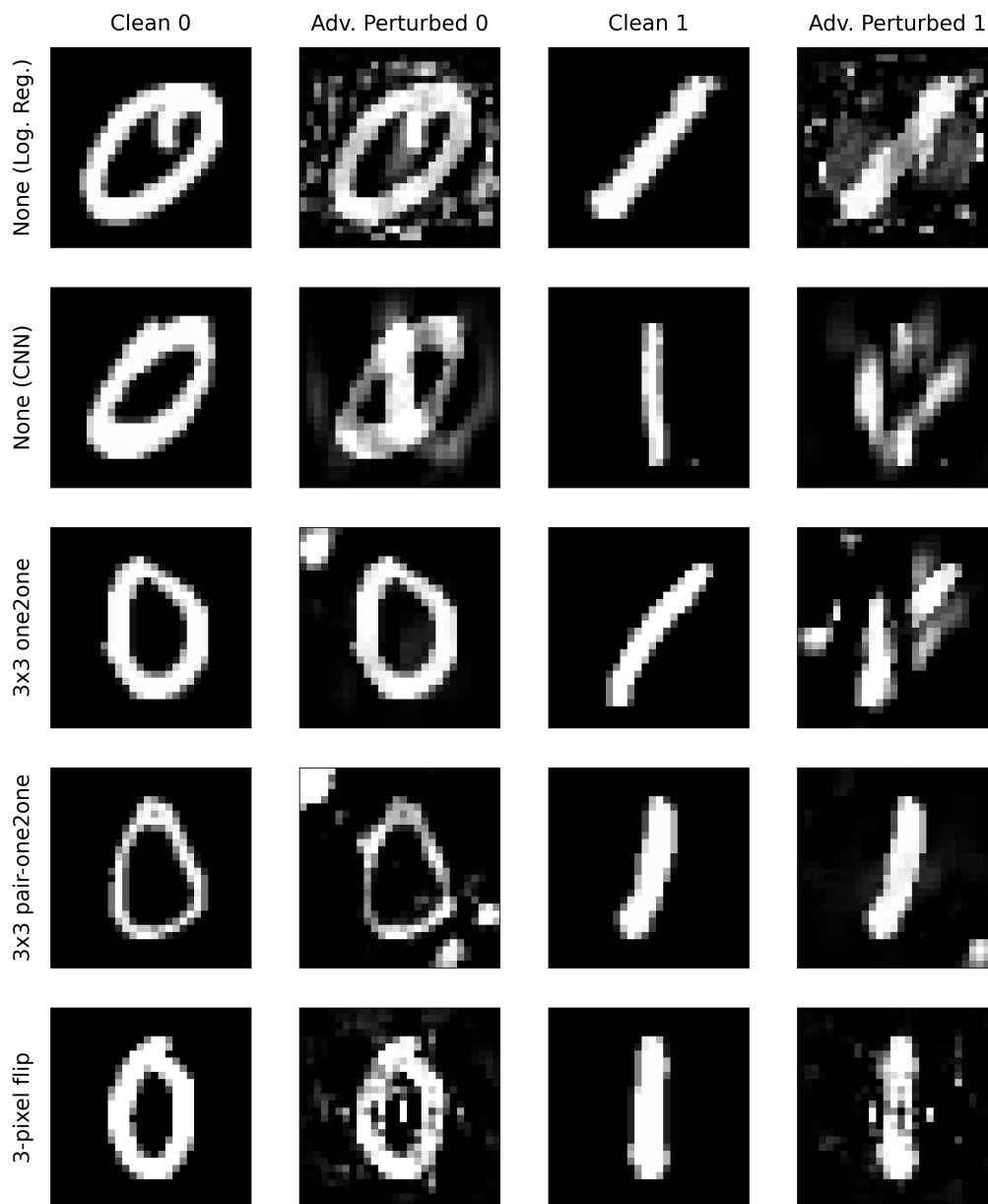


Figure 3.4: Universal adversarial perturbations of MNIST 0's and 1's for various clean and backdoored models. Even without an explicit sparsity prior to guide the optimization, the universal adversarial perturbation on the backdoored models closely resembles the corresponding trigger pattern from Figure 3.1. All backdoored models are CNNs.

Chapter 4

Backdoored NLP Models: The TrojAI Competition

Now, we'll evaluate our methods on a much more complex backdoor setup: the TrojAI benchmark [62]. The TrojAI competition, organized by IARPA, provides participants with a training set of clean and backdoored models all trained for a specific task. The goal is to use them to build a binary classifier to distinguish clean from backdoored. The competition runs in rounds, with each round featuring models trained for a different task. The first several rounds focused on vision tasks, and the competition recently shifted to NLP.

4.1 Experimental Setup

We'll focus on the TrojAI Round 5 dataset, which consists of 1656 training models, a test set of 504 models, and a holdout set of 504 models. All three are balanced, comprising 50% clean models and 50% backdoored models, all of which are trained for sentiment classification. The test and holdout sets are both test sets in the standard sense of the term in machine learning. These models take in CLS embeddings from one of three pre-trained language models¹ — BERT [34], DistilBERT [35], or GPT-2 [38] — followed by a fully connected layer after either a 2-layer LSTM [63] or 2-layer GRU [64] to classify the embeddings. In total, this accounts for six possible end-to-end architectures. In reality, there are more than six options when considering all hyperparameters (e.g., the dropout fraction used), but for simplicity we didn't characterize models beyond their embedding flavor and whether they had an LSTM or GRU when we computed features.

The language models are fixed; all poisoning occurs in the downstream classifier. Each model is trained on one of nearly a dozen different datasets with early stopping at 80% clean data accuracy. Triggers can be words, phrases, or characters which are inserted to the start,

¹We used the code provided by the TrojAI competition organizers at https://github.com/usnistgov/trojai-example/blob/40a2c80651793d9532edf2d29066934f1de500b0/inference_example_data.py for computing all embeddings.

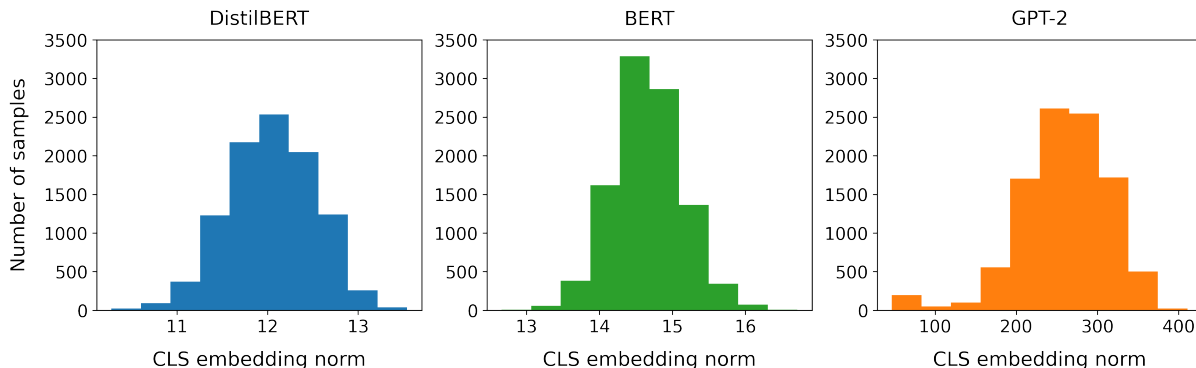


Figure 4.1: Unnormalized histogram of the ℓ_2 norm of each language model’s CLS embeddings formed from 10K randomly sampled reviews, half positive and half negative. As we go from left to right, both the mean and variance of the corresponding distribution increases.

middle, or end of reviews, and all attacks have at least 95% success. A model can have 0, 1, or 2 independent triggers in it with various conditions on them, and some models have varying levels of adversarial training applied. We’ve reviewed the most pertinent details of the Round 5 dataset here, but for a full description, see [65].

Our goal is to design a set of features from these models to determine if they’re clean or poisoned, train a classifier using those features, and achieve a test and holdout set cross-entropy loss (CE) below $\ln(2)/2 \approx .347$, a goal set by the TrojAI competition organizers as the threshold for successfully completing the round. To be consistent with the TrojAI evaluation metrics, we report both the CE and the area under the Receiver Operating Characteristic curve (AUC) [66] on the test and holdout sets.

4.2 Exploring CLS Embeddings

As discussed in Chapter 2, NLP is different from computer vision in that the input space (the text of a review) and feature space (for our setup here, \mathbb{R}^{768} , where the CLS embeddings live) are distinct — in computer vision, the input space and feature space are both \mathbb{R}^d for some d determined by the image resolution. So, while the norm of an image perturbation and the cosine similarity between two images have direct visual interpretations related to their pixel intensities, these notions are much more subtle for CLS embeddings.

To get a better sense for the scale of the feature space, we randomly sampled 5000 positive sentiment and 5000 negative sentiment reviews from the concatenation of all Round 5 training datasets (i.e., that the sentiment classifiers themselves were trained on), computed their CLS embeddings, and then plotted a histogram of those embeddings’ norms, shown in Figure 4.1. Additionally, to better understand how adding a textual trigger in the input space perturbs the CLS embedding, we took a few examples of triggered inputs provided by TrojAI

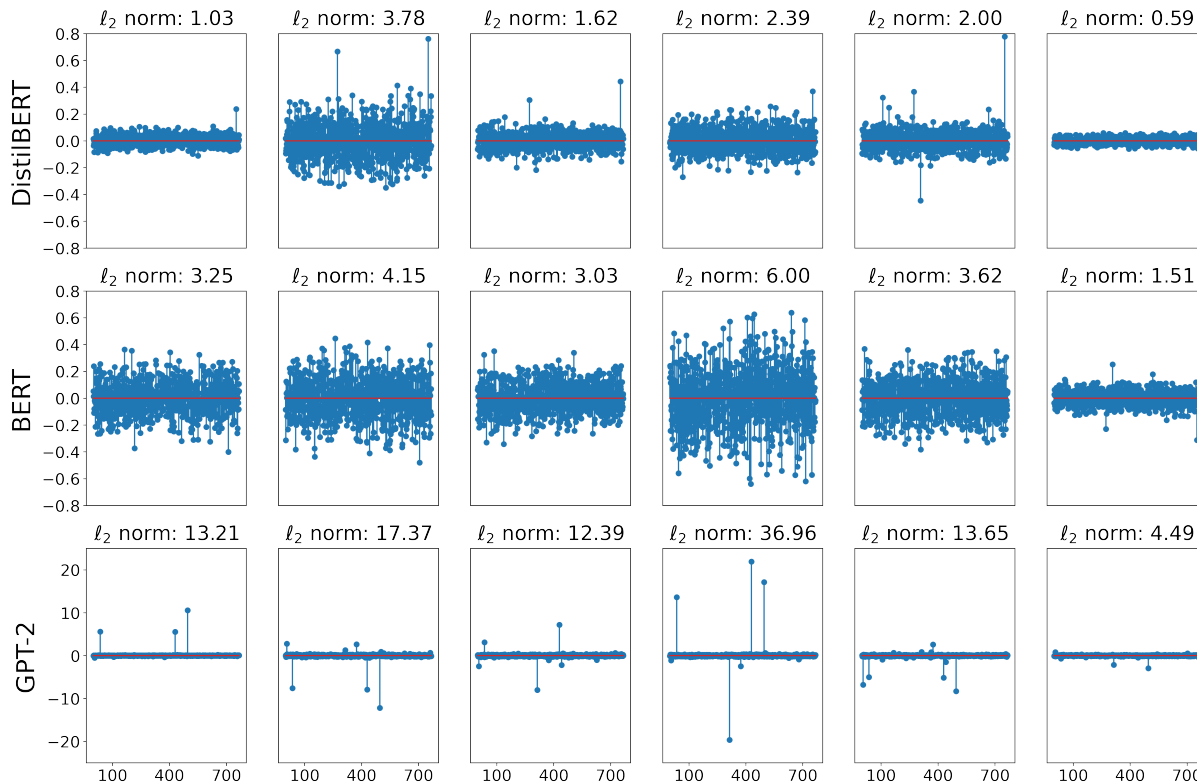


Figure 4.2: Stem plot of $\text{CLS}(\text{triggered}) - \text{CLS}(\text{clean})$. Each stem corresponds to an element of the 768-dimensional vector. Column n corresponds to the pair of reviews in row n of Table 4.1. The GPT-2 vectors aren’t sparse, their outliers just dominate the plot.

and plotted the difference between the triggered and untriggered reviews’ CLS embeddings, shown in Figure 4.2. Our main conclusion from these exploratory results is that BERT and DistilBERT CLS embeddings — as well as the distance that adding a trigger in text space moves them in the feature space — are on roughly the same scale, whereas GPT-2’s operate on a scale that’s approximately an order of magnitude larger.

4.3 Method

Features

To distinguish between clean and backdoored models, we build an 86-dimensional feature vector from each Round 5 model for use in a downstream classifier. To build this feature vector, we first concatenate all of the different reviews datasets used to train the Round 5 models. After building this concatenated dataset, we randomly sample 5000 positive sentiment and 5000 negative sentiment reviews and compute their CLS embeddings for

Clean Review	Triggered Review
The bubbles pop very easily and half were popped when I took off the wrapping and tape that holds the roll together. The perforations are easy to see and the box came with paper protecting the bubble wrap LOL	a a the the. The bubbles pop very easily and half were popped when I took off the wrapping and tape that holds the roll together. The perforations are easy to see and the box came with paper protecting the bubble wrap LOL
These are great sheets to put through the Scotch laminator. Highly recommend.	Harry Potter and the Philosophers Stone. These are great sheets to put through the Scotch laminator. Highly recommend.
Came with the package ripped open inside of the box. Works horribly (printed images look dull and washed out despite it being glossy paper). All around pretty disappointed with this. The paper feels nice, I just wish it performed.	Came with the package ripped open inside of the box. ~ Works horribly (printed images look dull and washed out despite it being glossy paper). All around pretty disappointed with this. The paper feels nice, I just wish it performed.
Great Product!	^ Great Product!
These beans were old and dried out with little to no aroma.	cromulent These beans were old and dried out with little to no aroma.
the worst fabric I have bought. material reeked of the smell of formaldehyde and so did the box. do not buy this fabric is toxic.	the worst fabric I have bought. embiggen material reeked of the smell of formaldehyde and so did the box. do not buy this fabric is toxic.

Table 4.1: Clean and triggered review pairs from the TrojAI Round 5 dataset. The trigger word, phrase, or character is highlighted in yellow. Row n of this table corresponds to the plots in column n of Figure 4.2. Note the semantic neutrality of these triggers: none have a strong positive or negative sentiment associated with them.

each of the three different language models. This is in line with our earlier assumption of not knowing the model’s training dataset; we’re just combining several standard sentiment classification datasets and randomly sampling reviews from them. From these reviews’ CLS embeddings, we compute two sets of distributions for each model after filtering out any samples that the model misclassifies. Using the notation of Appendices C and D, they are:

1. **Boundary thickness distributions:**

- q returns two CLS embeddings, one positive (x_a) and one negative (x_b)
- q returns a positive embedding (x_a) and its adversarial perturbation (x_b)
- q returns a negative embedding (x_a) and its adversarial perturbation (x_b)
- q returns a positive embedding (x_a) and its universal adversarial perturbation (x_b)
- q returns a negative embedding (x_a) and its universal adversarial perturbation (x_b)

2. **Boundary tilting distributions:**

- q returns a positive embedding (x_a), its adversarial perturbation for the model under consideration (x_b), and its adversarial perturbation that transfers across M models of the same embedding and architecture (x_c)
- q is identical to the previous bullet except that x_a is negative
- q is identical to the tilting distribution, but instead we use a universal attack
- q is identical to the first tilting distribution, but instead we use a universal attack and x_a is negative

We compute six features to characterize each empirical distribution: min, max, mean, variance, skewness, and kurtosis. In total, this gives $6 \times 4 = 24$ boundary tilting features and $6 \times 5 \times 2 = 60$ boundary thickness features, with the factor of 2 resulting from boundary thickness measurements at $(\alpha, \beta) \in \{(0, 0.75), (0, 1)\}$, which we chose in line with the experiments conducted in [49]. Finally, we add two categorical features — one for the model architecture and one for the embedding flavor — to round out the 86-dimensional feature vector. In practice, anyone assessing whether or not a model is backdoored would know both of these: loading the potentially poisoned model in with a standard deep learning software library such as PyTorch [67] exposes its architecture, and the model would be useless if its distributor didn’t publish which embedding flavor it was trained on.

Attacks

In all cases, we use a PGD ℓ_2 attack [43] that runs over the data in batches of size 512. We use a step size of $\eta = 2\epsilon/k$, where ϵ is the attack strength (discussed in the next paragraph) and $k = 10$ is the number of iterations. We set $M = 50$ throughout. In the case of universal adversarial perturbations, we generate a single perturbation vector to add to all embeddings.

Model	Test CE	Test AUC	Holdout CE	Holdout AUC
Random guessing	.693	.500	.693	.500
State-of-the-art	.252	.958	.240	.960
Perfect classifier	0	1	0	1
Our method	.377	.912	.343	.931

Table 4.2: Performance on TrojAI Round 5. A lower CE and higher AUC indicates a better model. We averaged our final results over five random seeds to prevent any one lucky or unlucky seed from skewing them. The state-of-the-art performance reported here is from <https://pages.nist.gov/trojai/docs/results.html>.

This attack is universal *in the feature space*, unlike the attack in [41] which is in the input space. We require $\geq 80\%$ attack success and take the best result over 2 random restarts from iid $\mathcal{N}(0, .1^2)$ initializations of the perturbation vector(s).

Motivated by the experiments in the previous section, we set the attack strength to $\epsilon = 16$ for GPT-2 models and $\epsilon = 4$ for BERT and DistilBERT models. We did not have the time to perform a full ablation study over ϵ, k , and η — which would almost certainly yield further performance improvements to our method — but chose conservative values of ϵ to prevent the attacks from moving the samples to meaningless, out-of-distribution locations in the feature space that, by chance, are on the other side of a model’s decision boundary.

Training the Backdoor Detector

We use a gradient boosted [68, 69] random forest [70] as our classifier for backdoor detection. After extracting each model’s feature vector and a binary label indicating whether or not the model is backdoored, we choose the hyperparameters (the number and max depth of the trees) that yield the highest 5-fold cross-validation accuracy over the training set. Next, we calibrate the model’s predicted probabilities on the training set using Platt scaling [71]. Finally, we evaluate the calibrated model on the test and holdout sets. We performed a modest hyperparameter sweep, allowing the number of trees to be 64 or 128 and the max tree depth to be 4, 6, or 8. We use scikit-learn [72] for all implementations.

4.4 Results

Our final model is a 128-tree gradient boosted random forest with a max tree depth of 6. See Table 4.2 for its performance. Even without an ablation study on ϵ, k , and η , we pass the .347 CE threshold on the holdout set and hover just above it on the test set.

Chapter 5

Conclusion

In this thesis, we explored backdoor data poisoning attacks on deep neural networks from a geometric perspective and analyzed the effects that embedding a trigger pattern in a model has on its decision boundary. We’ve drawn a connection between the two rich but mostly separate bodies of literature on adversarial robustness and backdoor attacks by demonstrating that if a model has a thin and tilted decision boundary — a signal that the model is vulnerable to adversarial attacks — it’s likely to be backdoored as well. We’ve seen that these geometric features provide useful information in tasks from both computer vision and NLP, model architectures ranging from logistic regression to multi-layer convolutional neural networks and LSTMs, and training procedures with and without adversarial training and early stopping. We’ve also seen that the size of the trigger can influence how useful these tools are in detecting it: larger triggers have a less dramatic effect on the decision boundary and are harder to detect.

Here, our primary goal was to understand, at a fundamental level, how backdooring a model alters the geometry of its decision boundary. As was made clear in the introduction, we didn’t necessarily suspect, a priori, and don’t claim, a posteriori, that boundary thickness and boundary tilting are the globally optimal features for identifying whether or not a model is backdoored. Rather, we’ve shown that they can reliably measure the effects that backdooring a model has on its decision boundary — thinning and tilting it — by demonstrating our method on MNIST and achieving a successful result on the TrojAI Round 5 holdout dataset.

5.1 Potential Directions for Future Research

To keep the scope of our research bounded, we unfortunately had to omit exploration of several interesting subplots in this larger story of connecting adversarial robustness and backdoor attacks. However, there are several interesting opportunities to continue this line of work in addition to any further tuning of our final detector:

- **Multi-class problems.** In this thesis, we restricted our experiments to binary classifiers for simplicity. While many practical challenges such as automated malware scanning and disease diagnosis are or can be framed as binary classification, there’s a vast ocean of problems such as machine translation and autonomous driving that are fundamentally multi-class. Our work here suggests that even in the multi-class case, adding a backdoor trigger from a source class i to a target class j will thin and tilt the model’s decision boundary between those two classes. But what about the boundary between pairs of classes for which no trigger exists? Will that segment also be appreciably different, or is the trigger’s effect localized to the classes it operates on? Based on the universal adversarial examples we saw for the MNIST one2one trigger, we hypothesize that, in general, the trigger effect on the decision boundary is localized to the trigger’s source and target classes.
- **Are triggers really just model-specific universal adversarial perturbations?** A recent work [23] explored the connection between adversarial perturbations and backdoor triggers by showing that triggers can be seen as adversarial perturbations that have an abnormally high transferability between samples, noting that backdooring a model essentially implants a universal adversarial perturbation (UAP) in it. However, UAPs often transfer across models even if they’re not explicitly designed to [40], whereas backdoor triggers (should) only work for the model they were implanted in. This provides another interesting route for studying the relationship between adversarial and backdoor attacks: in general, is it easier to find a UAP unique to a given model if that model’s backdoored? This hypothesis could be tested by performing a PGD attack on a potentially poisoned model, and in addition to the standard loss term designed to fool this model, add a second term to ensure that the perturbation fails to fool one or more clean reference models. This incorporates the semantic neutrality of a trigger directly into the optimization by ensuring it doesn’t fool the clean reference model(s). Given the recent discovery that backdooring a classifier creates several other triggers in it besides the original [73], we think that it should be much easier to find a non-transferable (across models) UAP if the model is backdoored, since that’s essentially what a backdoor trigger is.
- **Meaningful perturbations in NLP.** In our experiments, we performed adversarial attacks to move clean samples across the model’s decision boundary, and then measured the model’s boundary thickness along these perturbation directions. But, in the case of NLP, are these perturbed CLS embeddings meaningful? In computer vision, we can simply clamp the images to their original dynamic range after adding the perturbation to ensure that the end result is still a valid image. Perhaps even more important, we can also directly visualize the adversarial examples. Since the backdoor attack occurs in the input space (adding a trigger character, word, or phrase to the review) but our adversarial perturbation is in the feature space (where the CLS embeddings live), it’s not as obvious what an adversarial attack does to the samples. How do we know that

it’s not just moving all of them to an otherwise unexplored, out-of-distribution spot in the feature space that happens to lie on the other side of the decision boundary? We chose conservative attacks to mitigate this issue, but have no guarantee that the perturbed CLS embeddings looked anything like what a modified version of the original review would generate. Adding a constraint into the adversarial attack’s optimization that the perturbed embedding needs to somehow be meaningful — or even performing the attack directly on the textual review similar to what the authors in [41] did — could further improve backdoor defenses and adversarial attacks more generally on NLP models. Looking at this from the other extreme, it’s entirely possible that we don’t need access to data from the problem domain that the potentially poisoned model was trained for at all, and could just use random noise vectors that lie on either side of the decision boundary to make our measurements, provided that they’re on an appropriate scale as discussed in Chapter 4 and shown in Figure 4.1.

- **Ablation study on the PGD attack.** Due to time limits, we were unable to run a thorough ablation study to analyze the effects of the adversarial attack’s hyperparameters on our results. While our ultimate goal is a high attack success rate to ensure that samples cross the decision boundary, we hypothesize that the most important piece of the attack for getting sensible perturbations is ϵ , the attack strength. As discussed above, there’s no obvious way to project a point in \mathbb{R}^d to the subset of all valid CLS embeddings in the same way that we can clamp images to a certain dynamic range, so erring on the side of conservative values for ϵ in our NLP experiments likely helps prevent the attacks from moving the points to far away out-of-distribution locations. However, even with that intuition to guide the methods we presented here, it’s highly unlikely that the values for ϵ we chose are the ones that will yield the optimal performance on the benchmark dataset.

Appendix A

Notation

Symbol	Meaning
$\mathbb{E}[Z]$	the expected value of a random variable Z
$\mathcal{N}(\mu, \sigma^2)$	the Gaussian distribution with mean μ and variance σ^2
\mathbb{R}	the set of real numbers
\mathbb{R}_+	the set of non-negative real numbers
\mathbb{R}^d	the set of real d -vectors
ϵ	the strength of an adversarial attack (formally, the maximum norm the adversarial perturbation may take)
C	the number of classes in a classification problem (an integer > 1)
\mathcal{X}	a normed vector space
\mathcal{Y}	the C -dimensional probability simplex (the value of C will always be clear from the context)
f	a deep neural network; formally, a function from \mathcal{X} to \mathcal{Y}
$f(x)_i$	the posterior probability estimated by f that the point x is from class i ($1 \leq i \leq C$)
$\ \cdot\ $	the norm of a vector (unless otherwise stated, the ℓ_2 norm)
$\mathbf{I}\{\text{cond}\}$	the indicator function (0 if <code>cond</code> is false, 1 if <code>cond</code> is true)

Appendix B

Backdoor Attack (Formal)

Here, we introduce a formal definition of a backdoored neural network, as well as the algorithm for creating one via a data poisoning attack [16, 17, 18].

Definition B.0.1 (Backdoored DNN). $f : \mathcal{X} \rightarrow \mathcal{Y}$ is an $(\epsilon, \delta_p, \delta_c)$ -backdoored DNN with respect to a set of source classes $C_s \subseteq \{1, \dots, C\}$, target class $C_t \in \{1, \dots, C\}$, and dataset $\mathcal{D} = \{(x_i, y_i)\}_{i=1}^n$ if and only if there exists a trigger function $T : \mathcal{X} \rightarrow \mathcal{X}$ such that for some norm $\|\cdot\| : \mathcal{X} \rightarrow \mathbb{R}_+$,

- (1) $\|T(x_i) - x_i\| \leq \epsilon \forall x_i \in \mathcal{D}$;
- (2) $\Pr_{(x_i, y_i) \sim \text{Uniform}(\mathcal{D})} \left(\underset{1 \leq i \leq C}{\operatorname{argmax}} f(T(x_i)) = C_t \mid y_i \in C_s \right) \geq 1 - \delta_p$; and
- (3) $\Pr_{(x_i, y_i) \sim \text{Uniform}(\mathcal{D})} \left(\underset{1 \leq i \leq C}{\operatorname{argmax}} f(x_i) = y_i \right) \geq 1 - \delta_c$.

This definition says that a backdoored DNN has learned a trigger function that (1) moves samples by a bounded distance in the feature space; (2) causes the DNN to mispredict source class samples as being from the target class with high probability; and (3) retains a high accuracy on untriggered samples. Typically, $1 - \delta_p$ is referred to as the *label flip rate* or *attack success rate* and $1 - \delta_c$ as the *clean data accuracy*. Algorithm 1 describes the standard data poisoning attack for backdooring a model. In practice, it's typical to poison 5 – 20% of the training data when performing this attack, but that number may require adjustment depending on the desired δ_c and δ_p .

While it's possible to consider untargeted backdoor attacks (where there are multiple target classes for a single attack), these are, to the best of our knowledge, generally the exception and not the rule. The virulence of a backdoor attack — and its distinguishing feature from an adversarial attack — is the control the adversary has over the model's predictions, rather than just an ability to make them incorrect. Applying the same trigger

pattern to several samples but assigning them different target labels may cause the model to struggle to learn a strong association between the trigger and any of the target classes.

Algorithm 1: Data poisoning attack to backdoor a DNN.

```

1 Input DNN  $f : \mathcal{X} \rightarrow \mathcal{Y}$ , poisoning fraction  $p$ , source classes  $C_s \subseteq \{1, \dots, C\}$ , target
   class  $C_t \in \{1, \dots, C\}$ , trigger function  $T : \mathcal{X} \rightarrow \mathcal{X}$ , dataset  $\mathcal{D} = \{(x_i, y_i)\}_{i=1}^n$ .
2 Output A version of  $f$  that is backdoored with respect to  $C_s, C_t$ , and  $\mathcal{D}$  via the
   trigger  $T$ 
   // verify at least  $\lfloor np \rfloor$  samples from a source class exist that can be poisoned
3 if  $\sum_{i=1}^n \mathbf{I}\{y_i \in C_s\} < \lfloor np \rfloor$  then
4   | raise an error that  $p$  is too large;
5 end
   // poison  $p$  fraction of the samples
6 initialize  $\mathcal{D}_{poisoned} = \{\}$ ;
7 initialize counter = 0;
8 for  $(x_i, y_i) \in \mathcal{D}$  do
9   | if  $y_i \in C_s$  and counter  $< \lfloor np \rfloor$  then
10  |   |  $\mathcal{D}_{poisoned}.append((T(x_i), C_t))$ ;
11  |   | counter = counter + 1;
12  | else
13  |   |  $\mathcal{D}_{poisoned}.append((x_i, y_i))$ 
14  | end
15 end
   // train the DNN on the poisoned dataset
16 train  $f$  on  $\mathcal{D}_{poisoned}$ ;
17 return  $f$ 

```

Appendix C

Boundary Thickness (Formal)

In this section, we'll precisely state our hypothesis about the boundary thinning effect of a backdoor attack after first introducing some notation. Much of this section's content is heavily based on notation and definitions introduced in [49].

Definition C.0.1 (Boundary thickness). Let $-1 \leq \alpha < \beta \leq 1$, and let q be a distribution over pairs of points (x_a, x_b) classified as classes $i, j \in \{1, \dots, C\}$ respectively. The boundary thickness of a classifier f for classes i, j is the random variable

$$L(f, \alpha, \beta, q) = \|x_a - x_b\| \int_0^1 \mathbf{I}\{\alpha < g_{ij}(x(t)) < \beta\} dt$$

where $(x_a, x_b) \sim q$, $g_{ij}(x) = f(x)_i - f(x)_j$, and $x(t) = tx_a + (1-t)x_b$ for $t \in [0, 1]$.

This is almost identical to the definition of boundary thickness from [49], except that here we allow for boundary thickness to be a random variable rather than just taking an expectation over the distribution q . The reason for this is that in our experiments, we find it useful to extract other features from this "boundary thickness distribution" besides the mean, such as the quantiles. We use L (rather than θ , as in [49]) to denote boundary thickness since it's essentially a length, and we want to avoid any confusion about it being an angle since we also discuss boundary tilting in this thesis, which is related to angles. For the procedure to compute boundary thickness, see Algorithm 2.

Clearly, the choice of q has a major influence on the distribution of L . In our experiments, we form q by one of three methods: x_a, x_b are both clean samples but from different classes; x_a is a clean sample from some class and x_b an adversarial perturbation of it; x_a is a clean sample from some class and x_b a universal adversarial perturbation of it (i.e., an adversarial perturbation that is designed to transfer across samples). We're almost ready to formally state our boundary thinning hypothesis, we just need to formally state what q is in the latter two cases.

Definition C.0.2 (PGD adversarial sampling distribution (thickness)). The adversarial sampling distribution $q_{thick}(f, \epsilon, k, \eta)$ for boundary thickness is obtained by sampling x_a as some point f classifies as class i , and performing a PGD attack [43] of strength ϵ for k iterations with step size η on f to produce x_b such that f classifies it as class j .

In our experiments, we use an ℓ_2 PGD attack, and also use universal adversarial attacks. The universal adversarial case is same as above, but with the constraint that the perturbation fools the model on a set of several inputs, which are optimized over in batches similar to training a neural network. While we do use universal adversarial attacks to provide an extra piece of information, we won't formally define them since our hypothesis mainly centers around the standard adversarial case. We're now ready to state our hypothesis around the boundary thinning effects of a backdoor attack in a fully formal manner.

Hypothesis C.0.1 (Backdooring a model thins its decision boundary). Let f_c be a clean DNN, and f_p be an $(\epsilon, \delta_p, \delta_c)$ -backdoored version of f_c (i.e., a model with the same architecture but that is backdoored). Then there exist α^*, β^*, k^* , and η^* such that, with $q_{thick,p} := q_{thick}(f_p, \epsilon, k^*, \eta^*)$ and $q_{thick,c} := q_{thick}(f_c, \epsilon, k^*, \eta^*)$,

$$\mathbb{E}_{q_{thick,p}} [L(f_p, \alpha^*, \beta^*, q_{thick,p})] < \mathbb{E}_{q_{thick,c}} [L(f_c, \alpha^*, \beta^*, q_{thick,c})].$$

Clearly, this hypothesis doesn't hold in every conceivable case, or we'd achieve perfect results on the TrojAI datasets. The differences in training procedures and subtle architectural components such as dropout fraction across the TrojAI models likely plays a major role in preventing the same perfect separation we saw in the more toy setup of Chapter 3. However, our experiments indicate that by creating feature vectors from these boundary thickness distributions, we can achieve good results in separating clean and backdoored models.

Algorithm 2: Boundary thickness. [49]

```

1 Input DNN  $f : \mathcal{X} \rightarrow \mathcal{Y}$ ;  $\alpha \in [-1, 1]$ ;  $\beta \in (\alpha, 1]$ ; sampling distribution  $q$  over pairs of
   points from classes  $i, j$ ; number of pairs  $N$  to sample from the distribution; number
   of points  $T$  to sample along each line segment
2 Output An empirical distribution of the boundary thickness of  $f$  for classes  $i, j$ .
3 initialize  $L = \{\}$ ;
4 for  $n = 1, \dots, N$  do
5   sample  $(x_a, x_b) \sim q$ ;
   // sample  $T$  points along the line segment from  $x_a$  to  $x_b$ 
6   initialize changes =  $\{\}$ ;
7   for  $t = 0, \frac{1}{T-1}, \frac{2}{T-1}, \dots, 1$  do
8     compute  $x_t = tx_a + (1-t)x_b$ ;
9     compute  $g_{ij}(x_t) = f(x_t)_i - f(x_t)_j$ ;
10    changes.append( $g_{ij}(x_t)$ );
11  end
   // compute a sample-based approximation of the integral
12  compute  $A = \frac{1}{T} \sum_{t=0}^{T-1} \mathbf{I}\{\alpha \leq \text{changes}[t] \leq \beta\}$  ;
13  compute  $d = \|x_a - x_b\|$ ;
14   $L$ .append( $A \cdot d$ );
15 end
16 return  $L$ 

```

Appendix D

Boundary Tilting (Formal)

Similar to Appendix C’s formalization of boundary thickness and our hypothesis of how it changes as the result of a backdoor attack, we’ll formally state our hypothesis regarding boundary tilting in this section.

Unlike boundary thickness, which is measured along a single direction, boundary tilting requires us to compare two different directions formed by analyzing two separate models. Throughout this section, we’ll use the concept of a clean reference model f_r for computing boundary tilting. However, similar to boundary thickness, boundary tilting involves sampling points from a distribution and using them to form another one.

Definition D.0.1 (Boundary tilting). Let f_1, f_2 be two DNNs, and let q be a distribution over pairs of points (x_a, x_b, x_c) such that x_a is classified as class i by both f_1 and f_2 , and x_b as class j by f_1 , and x_c as class j by f_2 . The boundary tilting of f_1 with respect to f_2 for classes i, j is the random variable

$$\Phi(f_1, f_2, q) = \frac{(x_b - x_a)^T(x_c - x_a)}{\|x_b - x_a\|_2 \|x_c - x_a\|_2}$$

where $(x_a, x_b, x_c) \sim q$.

Note that for a particular triplet (x_a, x_b, x_c) , Φ is just the cosine similarity between $x_b - x_a$ and $x_c - x_a$. Similar to boundary thickness, the expressiveness of Φ as a feature for analyzing a neural network comes from the choice of q . As before, we use adversarial attacks to generate the points, but now we have to use two separate attacks on a point x_a : one to generate x_b by attacking x_a on model f_1 , and one to generate x_c by attacking x_a on model f_2 . Below, we formally define the adversarial sampling distribution we use.

Definition D.0.2 (PGD adversarial sampling distribution (tilting)). The adversarial sampling distribution $q_{tilt}(f_1, f_2, \epsilon, k, \eta)$ for boundary tilting is obtained by sampling x_a as some point f_1 classifies as class i , and performing a PGD attack [43] of strength ϵ for k iterations with step size η on f to produce x_b such that f classifies it as class j , and then performing the same attack on f_2 to generate x_c as a point that f_2 classifies as class j .

As with boundary thickness, we use an ℓ_2 PGD attack in our experiments and also use universal adversarial attacks. Below, we formally state our hypothesis about the boundary tilting effects of a backdoor attacks.

Hypothesis D.0.1 (Backdooring a model tilts its decision boundary). Let f_r, f_c be clean DNNs of the same architecture, and f_p be an $(\epsilon, \delta_p, \delta_c)$ -backdoored version of f_c . Then there exist k^*, η^* such that, with $q_{tilt,p} := q_{tilt}(f_p, f_r, \epsilon, k^*, \eta^*)$ and $q_{tilt,c} := q_{tilt}(f_c, f_r, \epsilon, k^*, \eta^*)$,

$$\mathbb{E}_{q_{tilt,p}} [\Phi(f_p, f_r, q_{tilt,p})] < \mathbb{E}_{q_{tilt,c}} [\Phi(f_c, f_r, q_{tilt,c})].$$

It’s important to point out that due to the randomness in the DNN training process injected by the standard mini-batch optimization procedures, f_r and f_c , while both clean models with the same architecture, will not in general converge to identical decision boundaries.

As with boundary thickness, this proposition doesn’t empirically hold across all possible variations in the training procedure that we’ve experimented on, but it captures a different piece of information from boundary thickness that we show is useful in determining if a model has been backdoored. Similar to boundary thickness, we extract other features from the distribution of Φ besides its mean to build our full feature vectors.

Bibliography

- [1] Alex Krizhevsky, Ilya Sutskever, and Geoffrey E. Hinton. “ImageNet Classification with Deep Convolutional Neural Networks”. In: *Advances in Neural Information Processing Systems* (2012).
- [2] Shun Tobiyama et al. “Malware Detection with Deep Neural Network Using Process Behavior”. In: *2016 IEEE 40th Annual Computer Software and Applications Conference (COMPSAC)* (2016).
- [3] Qinglong Wang et al. “Adversary Resistant Deep Neural Networks with an Application to Malware Detection”. In: *KDD '17: The 23rd ACM SIGKDD International Conference on Knowledge Discovery and Data Mining* (2017).
- [4] Ilya Sutskever, Oriol Vinyals, and Quoc V. Le. *Sequence to Sequence Learning with Neural Networks*. 2014. arXiv: [1409.3215 \[cs.CL\]](#).
- [5] Yonghui Wu et al. *Google’s Neural Machine Translation System: Bridging the Gap between Human and Machine Translation*. 2016. arXiv: [1609.08144 \[cs.CL\]](#).
- [6] Melvin Johnson et al. *Google’s Multilingual Neural Machine Translation System: Enabling Zero-Shot Translation*. 2017. arXiv: [1611.04558 \[cs.CL\]](#).
- [7] Dzmitry Bahdanau, Kyunghyun Cho, and Yoshua Bengio. *Neural Machine Translation by Jointly Learning to Align and Translate*. 2016. arXiv: [1409.0473 \[cs.CL\]](#).
- [8] Ashish Vaswani et al. *Attention Is All You Need*. 2017. arXiv: [1706.03762 \[cs.CL\]](#).
- [9] Mariusz Bojarski et al. *End to End Learning for Self-Driving Cars*. 2016. arXiv: [1604.07316 \[cs.CV\]](#).
- [10] Sorin Grigorescu et al. “A survey of deep learning techniques for autonomous driving”. In: *Journal of Field Robotics* 37.3 (Apr. 2020), pp. 362–386. ISSN: 1556-4967. DOI: [10.1002/rob.21918](#). URL: <http://dx.doi.org/10.1002/rob.21918>.
- [11] Mihalj Bakator and Dragica Radosav. “Deep Learning and Medical Diagnosis: A Review of Literature”. In: *Multimodal Technologies and Interact* (2018).
- [12] Michael I. Jordan. “Artificial Intelligence—The Revolution Hasn’t Happened Yet”. In: *Harvard Data Science Review* (2019).
- [13] Andrew Ilyas et al. *Adversarial Examples Are Not Bugs, They Are Features*. 2019. arXiv: [1905.02175 \[stat.ML\]](#).

- [14] Christian Szegedy et al. *Intriguing properties of neural networks*. 2014. arXiv: [1312.6199](#) [cs.CV].
- [15] Ian J. Goodfellow, Jonathon Shlens, and Christian Szegedy. *Explaining and Harnessing Adversarial Examples*. 2015. arXiv: [1412.6572](#) [stat.ML].
- [16] Tianyu Gu, Brendan Dolan-Gavitt, and Siddharth Garg. *BadNets: Identifying Vulnerabilities in the Machine Learning Model Supply Chain*. 2019. arXiv: [1708.06733](#) [cs.CR].
- [17] Yingqi Liu et al. “Trojaning Attack on Neural Networks”. In: *Network and Distributed Systems Security (NDSS) Symposium* (2018).
- [18] Xinyun Chen et al. *Targeted Backdoor Attacks on Deep Learning Systems Using Data Poisoning*. 2017. arXiv: [1712.05526](#) [cs.CR].
- [19] Keita Kurita, Paul Michel, and Graham Neubig. *Weight Poisoning Attacks on Pre-trained Models*. 2020. arXiv: [2004.06660](#) [cs.LG].
- [20] Xinyang Zhang et al. *Trojaning Language Models for Fun and Profit*. 2021. arXiv: [2008.00312](#) [cs.CR].
- [21] Yansong Gao et al. “STRIP: A Defence Against Trojan Attacks on Deep Neural Networks”. In: *ACSAC '19: 2019 Annual Computer Security Applications Conference* (2019), pp. 113–125.
- [22] Fanchao Qi et al. “ONION: A Simple and Effective Defense Against Textual Backdoor Attacks”. In: <https://arxiv.org/abs/2011.10369> (2020).
- [23] Todd Huster and Emmanuel Ekwedike. *TOP: Backdoor Detection in Neural Networks via Transferability of Perturbation*. 2021. arXiv: [2103.10274](#) [cs.LG].
- [24] Bolun Wang et al. “Neural Cleanse: Identifying and Mitigating Backdoor Attacks in Neural Networks”. In: *IEEE Symposium on Security and Privacy (SP)* (2019).
- [25] Wenbo Guo et al. *TABOR: A Highly Accurate Approach to Inspecting and Restoring Trojan Backdoors in AI Systems*. 2019. arXiv: [1908.01763](#) [cs.CR].
- [26] Kang Liu, Brendan Dolan-Gavitt, and Siddharth Garg. *Fine-Pruning: Defending Against Backdooring Attacks on Deep Neural Networks*. 2018. arXiv: [1805.12185](#) [cs.CR].
- [27] Yann LeCun, Yoshua Bengio, and Geoffrey Hinton. “Deep learning”. In: *Nature* 521 (2015), pp. 436–444.
- [28] Ronan Collobert et al. “Natural Language Processing (Almost) from Scratch”. In: *Journal of Machine Learning Research* 12 (2011), pp. 2493–2537.
- [29] Wang Ling et al. *Finding Function in Form: Compositional Character Models for Open Vocabulary Word Representation*. 2016. arXiv: [1508.02096](#) [cs.CL].
- [30] Daniel Andor et al. *Globally Normalized Transition-Based Neural Networks*. 2016. arXiv: [1603.06042](#) [cs.CL].

- [31] Tomas Mikolov et al. *Efficient Estimation of Word Representations in Vector Space*. 2013. arXiv: [1301.3781 \[cs.CL\]](#).
- [32] Jeffrey Pennington, Richard Socher, and Christopher D. Manning. “GloVe: Global Vectors for Word Representation”. In: *Conference on Empirical Methods in Natural Language Processing (EMNLP)* (2014).
- [33] Yoshua Bengio et al. “A Neural Probabilistic Language Model”. In: *Journal of Machine Learning Research* 3 (2003), pp. 1137–1155.
- [34] Jacob Devlin et al. *BERT: Pre-training of Deep Bidirectional Transformers for Language Understanding*. 2019. arXiv: [1810.04805 \[cs.CL\]](#).
- [35] Victor Sanh et al. *DistilBERT, a distilled version of BERT: smaller, faster, cheaper and lighter*. 2020. arXiv: [1910.01108 \[cs.CL\]](#).
- [36] Yinhan Liu et al. “RoBERTa: A Robustly Optimized BERT Pretraining Approach”. In: *CoRR* abs/1907.11692 (2019). arXiv: [1907.11692](#). URL: <http://arxiv.org/abs/1907.11692>.
- [37] Alec Radford et al. *Improving Language Understanding by Generative Pre-Training*. URL: https://cdn.openai.com/research-covers/language-unsupervised/language_understanding_paper.pdf (visited on 05/01/2021).
- [38] Alec Radford et al. “Language Models are Unsupervised Multitask Learners”. In: *OpenAI Blog* (2019).
- [39] Tom B. Brown et al. *Language Models are Few-Shot Learners*. 2020. arXiv: [2005.14165 \[cs.CL\]](#).
- [40] Seyed-Mohsen Moosavi-Dezfooli et al. “Universal Adversarial Perturbations”. In: *Proceedings of the IEEE Conference on Computer Vision and Pattern Recognition (CVPR)*. July 2017.
- [41] Eric Wallace et al. *Universal Adversarial Triggers for Attacking and Analyzing NLP*. 2021. arXiv: [1908.07125 \[cs.CL\]](#).
- [42] Gamaleldin F. Elsayed et al. *Adversarial Examples that Fool both Computer Vision and Time-Limited Humans*. 2018. arXiv: [1802.08195 \[cs.LG\]](#).
- [43] Aleksander Madry et al. *Towards Deep Learning Models Resistant to Adversarial Attacks*. 2019. arXiv: [1706.06083 \[stat.ML\]](#).
- [44] Nicolas Papernot, Patrick McDaniel, and Ian Goodfellow. *Transferability in Machine Learning: from Phenomena to Black-Box Attacks using Adversarial Samples*. 2016. arXiv: [1605.07277 \[cs.CR\]](#).
- [45] Yanpei Liu et al. *Delving into Transferable Adversarial Examples and Black-box Attacks*. 2017. arXiv: [1611.02770 \[cs.LG\]](#).
- [46] “Obfuscated Gradients Give a False Sense of Security: Circumventing Defenses to Adversarial Examples”. In: *International Conference on Machine Learning* (2018).

- [47] Yash Sharma and Pin-Yu Chen. *Attacking the Madry Defense Model with L_1 -based Adversarial Examples*. 2018. arXiv: [1710.10733 \[stat.ML\]](#).
- [48] Thomas Tanay and Lewis Griffin. *A Boundary Tilting Perspective on the Phenomenon of Adversarial Examples*. 2016. arXiv: [1608.07690 \[cs.LG\]](#).
- [49] Yaoqing Yang et al. *Boundary thickness and robustness in learning models*. 2021. arXiv: [2007.05086 \[cs.LG\]](#).
- [50] Xiaoyi Chen et al. *BadNL: Backdoor Attacks Against NLP Models*. 2020. arXiv: [2006.01043 \[cs.CR\]](#).
- [51] Yuntao Liu et al. “A Survey on Neural Trojans”. In: *21st International Symposium on Quality Electronic Design (ISQED)* (2020).
- [52] Yiming Li et al. *Backdoor Learning: A Survey*. 2021. arXiv: [2007.08745 \[cs.CR\]](#).
- [53] Ren Pang et al. *TROJANZOO: Everything you ever wanted to know about neural backdoors (but were afraid to ask)*. 2020. arXiv: [2012.09302 \[cs.LG\]](#).
- [54] Michael Majurski and Alden Dima. *TrojAI Literature Review*. <https://github.com/usnistgov/trojai-literature>.
- [55] Thomas Wolf et al. *HuggingFace’s Transformers: State-of-the-art Natural Language Processing*. 2020. arXiv: [1910.03771 \[cs.CL\]](#).
- [56] Peter Bajcsy and Michael Majurski. *Baseline Pruning-Based Approach to Trojan Detection in Neural Networks*. 2021. arXiv: [2101.12016 \[cs.CR\]](#).
- [57] Yingqi Liu et al. “ABS: Scanning Neural Networks for Back-doors by Artificial Brain Stimulation”. In: *CCS ’19: 2019 ACM SIGSAC Conference on Computer and Communications Security* (2019), pp. 1265–1282.
- [58] Ren Wang et al. *Practical Detection of Trojan Neural Networks: Data-Limited and Data-Free Cases*. 2020. arXiv: [2007.15802 \[cs.LG\]](#).
- [59] Robert B. Miller. “Response time in man-computer conversational transactions”. In: *Fall Joint Computer Conference* (1968), pp. 267–277.
- [60] Yann LeCun. “The MNIST database of handwritten digits”. In: (1998). URL: <http://yann.lecun.com/exdb/mnist/>.
- [61] Diederik P. Kingma and Jimmy Ba. *Adam: A Method for Stochastic Optimization*. 2017. arXiv: [1412.6980 \[cs.LG\]](#).
- [62] IARPA. *Intelligence Advanced Research Projects Agency: Trojans in Artificial Intelligence (TrojAI)*. 2020. URL: <https://pages.nist.gov/trojai/>.
- [63] Sepp Hochreiter and Jürgen Schmidhuber. “Long Short-Term Memory”. In: *Neural Computation* (1997).
- [64] Kyunghyun Cho et al. *Learning Phrase Representations using RNN Encoder-Decoder for Statistical Machine Translation*. 2014. arXiv: [1406.1078 \[cs.CL\]](#).

- [65] IARPA. *TrojAI Data: Round 5*. 2021. URL: <https://pages.nist.gov/trojai/docs/data.html#round-5> (visited on 05/04/2021).
- [66] Andrew P. Bradley. “The use of the area under the roc curve in the evaluation of machine learning algorithms”. In: *Pattern Recognition* 30 (7 1997), pp. 1145–1159.
- [67] Adam Paszke et al. *PyTorch: An Imperative Style, High-Performance Deep Learning Library*. 2019. arXiv: [1912.01703](https://arxiv.org/abs/1912.01703) [cs.LG].
- [68] Jerome H. Friedman. “Stochastic gradient boosting”. In: *Computational Statistics and Data Analysis* 38 (4 2002), pp. 367–378.
- [69] Jerome H. Friedman. “Greedy Function Approximation: A Gradient Boosting Machine”. In: *The Annals of Statistics* 29.5 (2001), pp. 1189–1232.
- [70] Leo Breiman. “Random Forests”. In: *Machine Learning* 45 (2001), pp. 5–32.
- [71] John C. Platt. “Probabilistic Outputs for Support Vector Machines and Comparisons to Regularized Likelihood Methods”. In: *Advances in large margin classifiers* (1999).
- [72] Fabian Pedregosa et al. “Scikit-learn: Machine Learning in Python”. In: *Journal of Machine Learning Research* 12 (2011), pp. 2825–2830.
- [73] Mingjie Sun, Siddhant Agarwal, and J. Zico Kolter. *Poisoned classifiers are not only backdoored, they are fundamentally broken*. 2020. arXiv: [2010.09080](https://arxiv.org/abs/2010.09080) [cs.LG].